USE OF HIGH PERFORMANCE COMPUTING TO CONDUCT FINE SCALE NUMERICAL SIMULATIONS OF ATMOSPHERIC FLOW IN COMPLEX TERRAIN

D. J. Grove*
U. S. Army Research Laboratory
Aberdeen Proving Ground, MD 21005-5067

P. A. Haines
U. S. Army Research Laboratory
White Sands Missile Range, NM 88002

W. Sun
Purdue University
West Lafayette, IN 47907-2051

W. Hsu
National Taiwan University
Taipei, Taiwan

ABSTRACT

Numerous observational and modeling studies have revealed a wide variety of atmospheric flows around, through and above terrain obstacles. Most such studies, however, have considered fairly simple terrain such as an isolated summit or an infinite perpendicular barrier exposed to uniform or relatively simple atmospheric conditions. Real terrain and real atmospheric conditions are considerably more complex than those used in the above mentioned studies and the resulting atmospheric flow is even more complicated and diverse.

This paper highlights the results from a series of high resolution (1.0 km grid spacing) numerical simulations using the National Taiwan University (NTU) / Purdue model for a variety of flow situations such as hydraulic jump, lee waves, juxtaposition of supercritical and sub-critical flows, etc. To complete these computations in a reasonable amount of time, the NTU/Purdue model simulations were run on a 1024-node Linux Networx Evolocity II cluster at the Army Research Laboratory (ARL) Major Shared Resource Center (MSRC). The parallelized NTU/Purdue model's scalability characteristics were evaluated for a fixed grid size, with the number of processors ranging from 4 to 128; the model scales very well up to at least 128 processors on the ARL MSRC's Linux cluster.

1. INTRODUCTION

Much of the White Sands Missile Range (WSMR) lies to the lee of the Organ and San Andres Mountains in southern New Mexico. The Organ Mountains include a rugged quasi-circular 1500 m high massif with a diameter of about 10 km. It is connected to a narrow and remarkably steep 1 to 1.5 km SE-NW oriented ridge. The ridge, in turn, connects to the approximately 100 km long south-to-north oriented barrier of the San Andres Mountains. Several passes and one additional massif complicate the San Andres barrier. Because of the variations in elevation, it is possible during a given situation at WSMR to have both sub- and super-critical flows in juxtaposition, greatly complicating the resulting flow and presenting significant challenges to numerical forecasting models.

While many U. S. Army missions are significantly impacted by the highly variable weather conditions in and around complex terrain such as at WSMR, the Army's ability to accurately forecast and diagnose such conditions remains limited. To better understand and to evaluate and improve the capabilities of numerical models to forecast the effects of terrain on weather conditions, the ARL collected surface data from five instrumented towers (10 m in height) positioned in the lee of the Organ Mountains during the first three months of 2004. In addition, data from the WSMR Surface Automated Meteorological System (SAMS) and other nearby surface stations such as the Remote Automated Weather Stations (RAWS) and the wind profiling radar at White Sands were collected. The total data set enables meso-β (2 to 20 km) and -γ (200 m to 2 km) scale depiction of the wind flow in the lee of the Organ Mountains; this is augmented in the vertical direction using horizontal and vertical wind component data from the White Sands wind profiling radar.

The following sections provide a brief description of the numerical forecasting model employed, comparisons of the numerical results with the observations, details of the model's scalability characteristics, and a discussion of the potential for future applications.

Report Documentation Page

Form Approved
OMB No. 0704-0188

Public reporting burden for the collection of information is estimated to average 1 hour per response, including the time for reviewing instructions, searching existing data sources, gathering and maintaining the data needed, and completing and reviewing the collection of information. Send comments regarding this burden estimate or any other aspect of this collection of information, including suggestions for reducing this burden, to Washington Headquarters Services, Directorate for Information Operations and Reports, 1215 Jefferson Davis Highway, Suite 1204, Arlington VA 22202-4302. Respondents should be aware that notwithstanding any other provision of law, no person shall be subject to a penalty for failing to comply with a collection of information if it does not display a currently valid OMB control number.

1. REPORT DATE **01 NOV 2006**	2. REPORT TYPE **N/A**	3. DATES COVERED **-**

4. TITLE AND SUBTITLE **Use Of High Performance Computing To Conduct Fine Scale Numerical Simulations Of Atmospheric Flow In Complex Terrain**	5a. CONTRACT NUMBER 5b. GRANT NUMBER 5c. PROGRAM ELEMENT NUMBER
6. AUTHOR(S)	5d. PROJECT NUMBER 5e. TASK NUMBER 5f. WORK UNIT NUMBER
7. PERFORMING ORGANIZATION NAME(S) AND ADDRESS(ES) **U. S. Army Research Laboratory Aberdeen Proving Ground, MD 21005-5067**	8. PERFORMING ORGANIZATION REPORT NUMBER
9. SPONSORING/MONITORING AGENCY NAME(S) AND ADDRESS(ES)	10. SPONSOR/MONITOR'S ACRONYM(S) 11. SPONSOR/MONITOR'S REPORT NUMBER(S)

12. DISTRIBUTION/AVAILABILITY STATEMENT
Approved for public release, distribution unlimited

13. SUPPLEMENTARY NOTES
See also ADM002075., The original document contains color images.

14. ABSTRACT

15. SUBJECT TERMS

16. SECURITY CLASSIFICATION OF:			17. LIMITATION OF ABSTRACT	18. NUMBER OF PAGES	19a. NAME OF RESPONSIBLE PERSON
a. REPORT **unclassified**	b. ABSTRACT **unclassified**	c. THIS PAGE **unclassified**	**UU**	**26**	

Standard Form 298 (Rev. 8-98)
Prescribed by ANSI Std Z39-18

2. NUMERICAL FORECASTING MODEL

The NTU/Purdue nonhydrostatic numerical model, hereafter referred to as the NTU/P model, has been under development over the last 8 years to predict atmospheric motions and conditions for both the mesoscale (200 m to 200 km) and large scale turbulence (20 m to 200 m) scales. The model explicitly solves the fully compressible nonhydrostatic system of equations (Hsu and Sun, 2001) and builds on the proven success of a preceding hydrostatic numerical model (Chern, 1994, Sun et al. 1991, Sun and Chern, 1993, Haines et al., 1997). The vertical coordinate of the model is defined as:

$$\sigma = \frac{p_0(z) - p_0(z_{top})}{p_0(z_{surface}) - p_0(z_{top})} \ , \qquad (1)$$

where p_0, the reference atmosphere pressure, is strictly a function of height. Although this vertical coordinate appears to be the usual σ-pressure coordinate used in many hydrostatic models, the pressure in (1) is not a function of time, so the position of each grid point is fixed in time. Hence, the model employs, strictly speaking, a σ-z coordinate. The advection terms are calculated with the Sun (1993) advection scheme. The diffusion process is parameterized through a level 2.5 turbulence scheme. Density is a prognostic variable which gives the advantage is that there is no diabatic term in the density prognostic equation.

The pressure field is diagnosed through the equation of state for a perfect gas,

$$p = \rho R T \ , \qquad (2)$$

where ρ is density, T is temperature, and R is the gas constant. Equivalent potential temperature (θ_e) is used as the prognostic variable in the heat equation, with θ_e defined as:

$$\theta_e = \theta + \left(\frac{\theta}{T}\right)\frac{L_v}{c_p} q_v \ , \qquad (3)$$

where θ is potential temperature, c_p is the specific heat at constant pressure, q_v is the specific humidity of water vapor, and L_v is the latent heat of vaporization. The total specific humidity, $q_w = q_v + q_l$ (where q_l is the liquid water content) is also a semi-conservative quantity in the absence of precipitation.

The fully explicit solution system employed by the NTU/P model is simple, memory-efficient, and very accurate for high frequency waves. Thus, it can provide a good comparison basis for the implementation of semi-implicit or other more time-efficient schemes to ensure their accuracy. As with many forecasting models, the Arakawa-C grid is employed, with density and vertical velocity also staggered (with respect to each other) in the vertical direction. The model uses a two-tier forward-backward solution procedure that is neutral in time with respect to both sound waves and internal gravity waves. This forward-backward scheme for sound and gravity waves means that the new solution values corresponding to the current time immediately replace those of the preceding time during the calculation so that only one storage array is required. Therefore, this scheme uses only half of the memory space required by centered finite difference schemes typically employed in numerical forecasting models. In addition, this scheme produces no computational modes (i.e., numerical noise), thus avoiding the need for a time filter. The compressible set of equations admits fast sound waves necessitating a small time step for their solution. The consequences of the small time step are mitigated through the use of a time-splitting technique (Gadd, 1978) in which the time integration is split into three stages; the corresponding time steps depend on the physical time scales of the calculated terms which involve advection, sound and other fast waves, and diffusion. The details of the numerical scheme are presented in Hsu and Sun (2001). The NTU/P model software package has been fully parallelized using Message Passing Interface (MPI) library routines.

3. OBSERVATION DETAILS

From January into March 2004 the ARL set up five instrumented towers (10 m in height) in the lee of the Organ Mountains. Each tower measured and recorded the wind direction and wind speed at a height of 10 m above ground level, as well as pressure, humidity, and temperature at a height of 2 m above the ground. The pressure instruments used were inter-compared, yielding an accuracy of +/- 10 pascals or better. Meanwhile, ARL also collected data from several of the nearby WSMR SAMS and RAWS sites to provide a fairly detailed picture of the surface air flow in and around the Organ Mountains. During the three-month observation time period, there were several down-slope wind storms and a variety of blocked-flow episodes. Besides the collected surface data, we obtained the vertical and horizontal wind profiles recorded by the two collocated wind profiling radars at White Sands that are situated about 15-20 km downwind of the mountains. These radar systems provide data coverage from about 500 m above their ground elevation (4000 feet) to about 17 km above sea level.

4. SIMULATION RESULTS

4.1 Lee Waves / Hydraulic Jump

On January 25, 2004, a down-slope wind storm occurred along the lee of the Organ and San Andres Mountains; it included the formation of a train of lee

waves which extended downwind across the Tularosa Basin and a hydraulic jump just to the lee of the mountains that was well-observed by the ARL and SAMS pressure sensors. These storms occur occasionally at White Sands, but this day's storm was especially noteworthy because the surface and other observations were able to document many of its facets, thus enabling detailed comparisons with the numerical model results.

To simulate this case, the NTU/P model's three-dimensional (3D) grid was set up with a vertical spacing of 300 m and a horizontal resolution of 1 km. Digital Terrain Elevation Data (DTED) level 2 terrain data was used to generate (via bi-linear interpolation) a 201 x 201 grid (with 1 km spacing) for a 200 km x 200 km region centered just to the east of the San Augustine Pass. Initially, when the NTU/P model's terrain smoothing algorithm was employed to eliminate two-delta x variations and to smooth the terrain at the periphery of the model domain, we found that the maximum terrain heights were somewhat less than the actual terrain. By experimenting, we found that a two step process could result in maximum terrain heights quite close to the actual values. In the first step, each initial terrain height above 1400 m was increased by an amount equal to 40% of the difference between the initial terrain height and 1400 m. Then, in the second step, the resulting combination of adjusted and unadjusted terrain heights was smoothed. Of course, it was not possible to obtain the maximum height of very narrow features such as the Organ Mountains ridge, but as can be seen in Fig. 1 the maximum height of the Organ Mountains (2720 m) and of the southern massif of the San Andres Mountains (2189 m) are well replicated in the terrain field used in this study. At the same time, the horizontal breadths of the mountains and the height of the Tularosa basin are preserved and agree extremely well with the real terrain.

Figure 2 reveals the details of the El Paso, Texas sounding at 12Z (1200 UCT) on 25 January 2004. Note the strong inversion at about 600 hPa or about 4000 m above sea level (asl). Calculated values of the Scorer Parameter (Scorer, 1949) are shown in this figure for the areas below and above the inversion. It is known that a significant decrease of the Scorer Parameter in the vertical when gravity waves are likely should result in lee waves downstream from the terrain. The model results and observations all strongly support the occurrence of lee waves.

Using the sounding shown in Fig. 2, along with the assumptions of a no-slip surface and no Coriolis force, the NTU/P model was initialized and integrated for three hours. The simulation results are presented in Figs. 3 through 6. Figure 3 compares the model-predicted wind field with the recorded observations at 0800 local time (1500 UCT) on January 25, 2004. In this figure, the

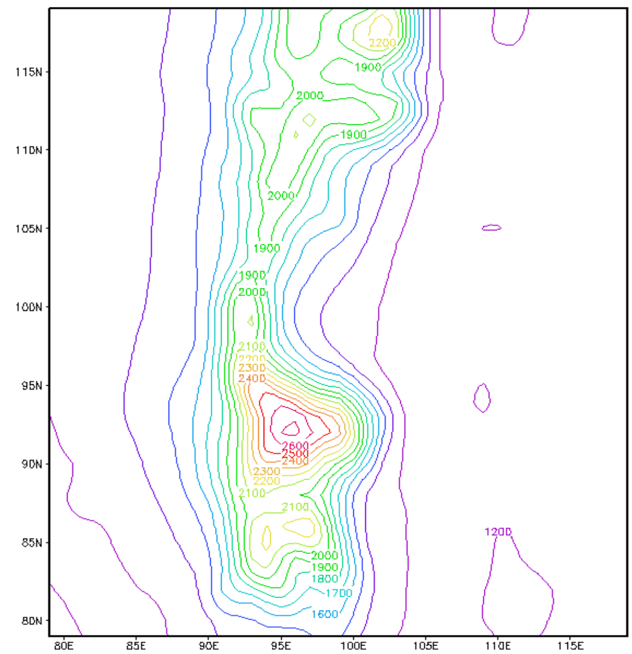

Fig. 1: NTU/P model domain terrain field for the central part (i:80-120; j:80-120) of the 201x201 grid; terrain heights are in meters above sea level and contours are every 100 m.

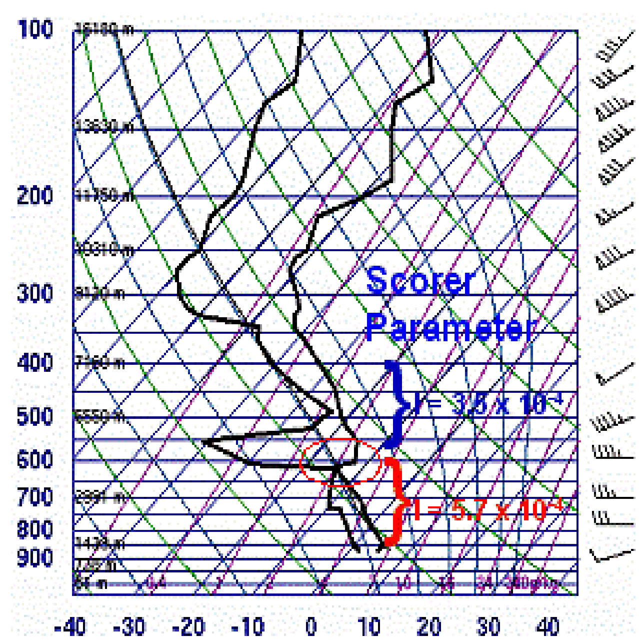

Fig. 2: El Paso, TX sounding for January 25, 2004 at 12Z.

NTU/P model's surface wind field is represented by the wind vectors, which indicate a strong down-slope flow on the lee side of the Organ and San Andres Mountains. In a band oriented mainly south-to-north just east of the mountains, the model's surface winds abruptly lessen and then either reverse (from W to E) or remain considerably diminished; this hydraulic jump corresponds to the strong

adverse pressure gradient shown by the pressure perturbations. The transitions to reversed flow appear to the North East of the higher terrain areas such as the Organ Mountains and the higher terrain to the north of the WSMR post. The reversed regions are about 5 km wide; to the east of the reversed region, the model surface winds return to westerly but are not as strong as in the strong down-slope flow area just to the lee of the Organ Mountains. Still farther to the east, about 20-25 km east of the mountain chain, there is another diminished or reversed wind region which is not as continuous or strong as that immediately to the lee of the mountains.

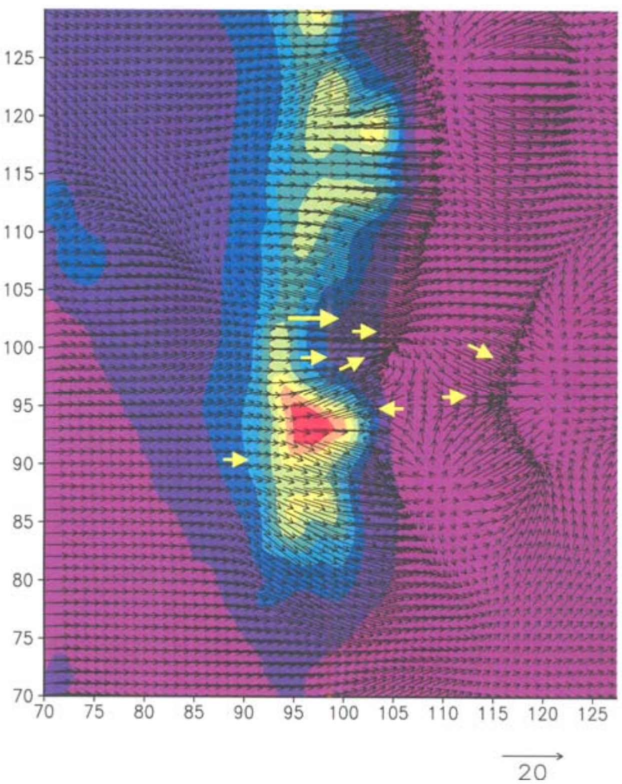

Fig. 3: Predicted surface wind field from the NTU/P model simulation of the January 25 down-slope wind storm case at WSMR (after 3 hours of model integration); yellow arrows indicate the observed wind field.

The observed winds are shown by the yellow arrows in Fig. 3. The model's wind field agrees quite closely with the actual wind field, except that the observed winds at the San Augustine Pass are stronger than the model's prediction. This pass is approximately 1 to 2 km wide. While the model's grid spacing is 1 km, its effective resolution is no better than 5 km. Hence, we expect that a numerical model will require a grid spacing of about 300-400 m or less to adequately resolve the wind flow at the San Augustine Pass.

Figure 4 compares the model's predicted surface nonhydrostatic pressure perturbations with the observed pressure perturbations from the ARL and SAMS pressure sensors. The colored contour lines show the NTU/P model's 3 hour forecast of the surface pressure perturbations; the values range (approximately) from 0 to -200 pascals (-2 hPa). There is a band of maximum negative perturbation pressure running south-to-north along the lee side of the Organ Mountains. A little farther east, the model shows a band of little or no perturbation pressure. Even farther east, there is another band of negative perturbation pressure. These model-predicted bands continue across the Tularosa basin in connection with the lee waves.

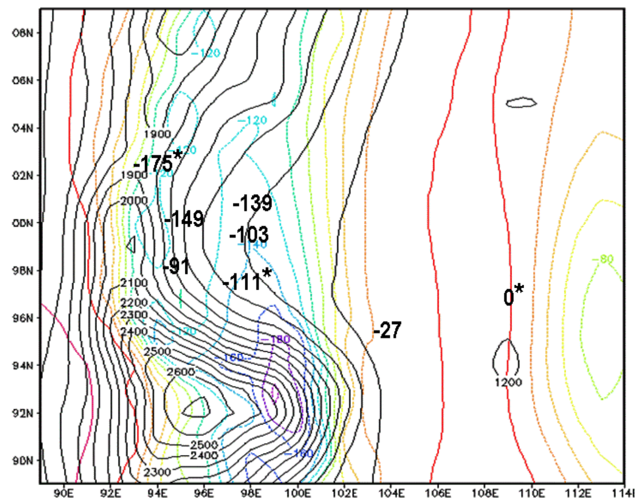

Fig. 4: Predicted surface pressure perturbations (color contours, in pascals) from the NTU/P model simulation of the January 25 down-slope wind storm case at WSMR; bold numbers (in black) indicate the observed pressure perturbations from the ARL and SAMS observations.

The observations shown in Fig. 4 include the ARL instrumented towers and the SAMS sites (indicated by *) in this area. The observed pressure perturbations were very carefully extracted through pressure reduction to a common datum plane at 1295 m. With the exception of the observation at the San Augustine Pass, the height of this plane minimized the vertical distance over which pressure reduction was done for the observations, consequently minimizing the error of the extracted pressure perturbations.

Except for the San Augustine site, the model's predicted wind field and pressure perturbation bands are in good agreement with the observations. In addition, the model's predicted pressure perturbation compares well with the observation from the Oro Grande Gate SAMS which is located far to the east of the area shown in Fig. 4.

Vertical cross-sections of vertical and horizontal wind components and the pressure perturbations support the occurrence of a hydraulic jump in conjunction with the wind reversal and adverse pressure gradient shown in

Figs. 3 and 4. Figure 5 shows a west to east cross section of the NTU/P model's predicted vertical velocity field for 0800 local time (1500 UCT) on January 25, 2004, located north of the WSMR post, approximately intersecting the San Augustine Pass and, more importantly, coinciding with the location of the White Sands wind profiling radar (shown by the dark vertical line in Fig. 5). The model prediction shows partially trapped lee waves extending eastward across the Tularosa Basin. The maximum vertical velocities are greater than 3 m/s. Using the Scorer Parameters calculated from the El Paso sounding, the theoretical wavelength of 13-14 km compares fairly closely to the model-predicted wavelength of around 14-15 km. The observed lee waves are well represented by the model's surface winds, are in fairly good agreement with the wind profiler observations, and are consistent with a decrease (with height) in the Scorer Parameter, defined as:

$$l^2 = \frac{N^2}{U^2} - \frac{1}{U}\frac{d^2U}{dz^2}, \qquad (4)$$

where U is the horizontal velocity (m/s) and N is the Brunt-Väisälä frequency (1/s).

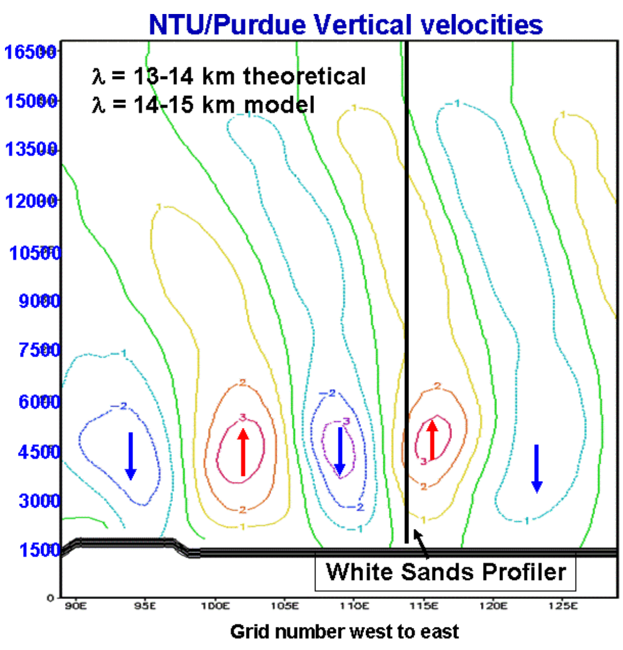

Fig. 5: NTU/P model-predicted vertical velocity field (m/s) at 0800 local time on January 25, 2004 along a west to east cross-section that intersects with the location of the White Sands (vertical black line) wind profiling radar.

Figure 6 compares the NTU/P model's predicted vertical velocities with the White Sands wind profiler data on January 25, during approximately the same time interval (0700 – 0900 local time). In this figure, the y-axis represents the height (in meters) asl, while the x-axis is the vertical velocity (in m/s). The model's vertical velocity profiles are shown by continuous color lines; the corresponding times are shown in the legend on the upper right hand side of this figure. The model shows two peaks in vertical velocity: one maximum at about 4500 m, and the second at about 12000 m. The model predicted a steady drop in the lower peak's vertical velocities from 0730 to 0830, with essentially no change between 0830 and 0900, while the upper peak's vertical velocities were steadier over this same time period.

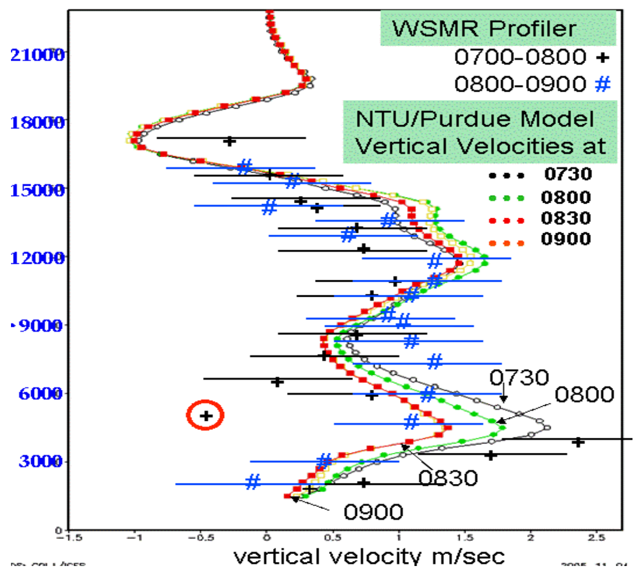

Fig. 6: Comparison of the NTU/P model-predicted vertical velocity profiles with the observed velocity profiles at the White Sands wind profiling radar location on January 25, 2004.

In Fig. 6, the vertical velocity profiles recorded by the White Sands wind profiler are shown by the black pluses and blue pound signs. These are the mean values, respectively, for the "0700-0800" and "0800-0900" local time periods; what is shown has been smoothed by using a running 5 point mean value, because the individual point values are quite noisy. The wind profiler is believed to have an accuracy of +/- 0.5 m/sec, so the corresponding error bars were included for each observed value. The observations show that the lower maximum's vertical velocities decrease going from hour 1 to 2 but the upper maximum's vertical velocities are roughly the same. It should be mentioned that the profiler's winds are obtained from processing of radial components along three beams that are not quite vertically oriented so the obtained value is probably more representative of the vertical velocity over a volume of space rather than being a point measurement. Despite these limitations, the NTU/P model's predictions of vertical velocity are in general agreement with the observations at the White Sands profiler site.

4.2 Blocking Effects / Down-Slope Winds

The blocking effects of mountains on air flow have been studied for years. However, most studies have been conducted with either an idealized mountain or for synoptic-mesoscale systems due to the difficulties of collecting very high resolution data or even developing a reliable forecasting model. Also, until recently, computational limitations have prevented the numerical solution of this high-resolution, three-dimensional problem in a reasonable amount of time. The results from this study indicate that the high resolution NTU/P model is capable of reproducing the details of the flow in very pronounced terrain under different prevailing wind conditions. Using the same grid and terrain data as in the preceding case, the model was initialized with the El Paso, Texas sounding at 12Z on January 19, 2004 (see Fig. 7) and integrated for three hours.

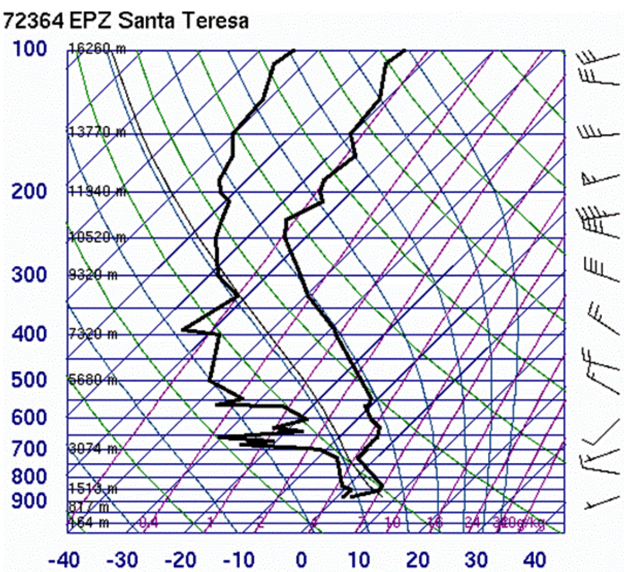

Fig. 7: El Paso, TX sounding for January 19, 2004 at 12Z.

Because of the variation in terrain heights, some of the areas to the lee of the Organ Mountains on January 19 are subject to blocking, while the flow for other areas is supercritical and down-slope winds develop. The model-predicted overall flow situation is quite complex, as indicated by Fig. 8. The model-predicted wind field is represented by the colored vectors. The low level wind field is quite complex; there is blocked flow (BF) in the lee of the Organ Mountains, but also down-slope wind (DW) flow on the south side of the Organs and to the north of the WSMR post.

The Froude Number (defined in the upper right hand corner of Fig. 8) provides a good measure of whether air will go over or around a terrain obstacle. Because of the different height scales, in this case the Froude Number is less than 1 for flow trying to go directly over the Organ Mountains, but is greater than 1 elsewhere so the flow can go over the terrain. Hence, we have a juxtaposition of sub and super-critical flow, which helps produce the complexities shown. Note that the observations generally confirm the model predictions, although the observed winds at the San Augustine Pass are stronger than those given by the model.

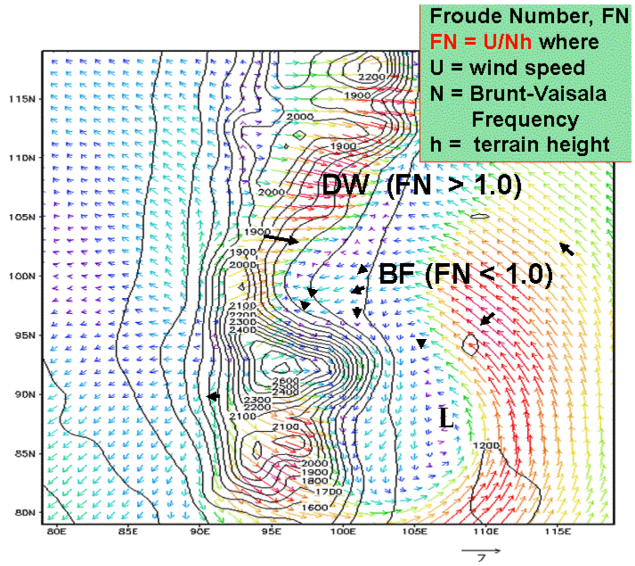

Figure 8: Predicted surface wind field (color vectors) from the NTU/P model simulation for January 19, 2004 at WSMR (after 3 hours of model integration); black arrows indicate actual observations (10 m above the ground).

The blocking effect becomes more pronounced when the Froude Number is less than 0.5, so we decided to investigate the case for a 5 m/s westerly prevailing wind. Using the same grid and terrain data as in the preceding cases, the model was initialized with a 5 m/s westerly wind, uniform stratification, and integrated for several hours. Figure 9 shows the resulting model-predicted surface wind field and surface streamlines; the color contour regions in this figure indicate the terrain levels.

In Fig. 9(a) we can see that the surface wind is blocked by the Organ Mountains and produces a counter-gradient flow on the windward side (near x = 95, y = 95), stronger wind at San Augustine Pass (near x = 95 and y = 102), and lee vortices (at x = 105, and y = 35, 85), as well as a strong down-slope wind on the lee side, all of which are also clearly indicated by the surface streamlines in Fig. 9(b).

The blocking effects of the WSMR terrain, particularly in the lee of the Organ Mountains, have been shown in SAMS and other data (Grove and Haines, 2002). Grove and Haines noted that the wind flow shown by the SAMS stations was consistent with the formation of a lee vortex. However, the number of SAMS stations

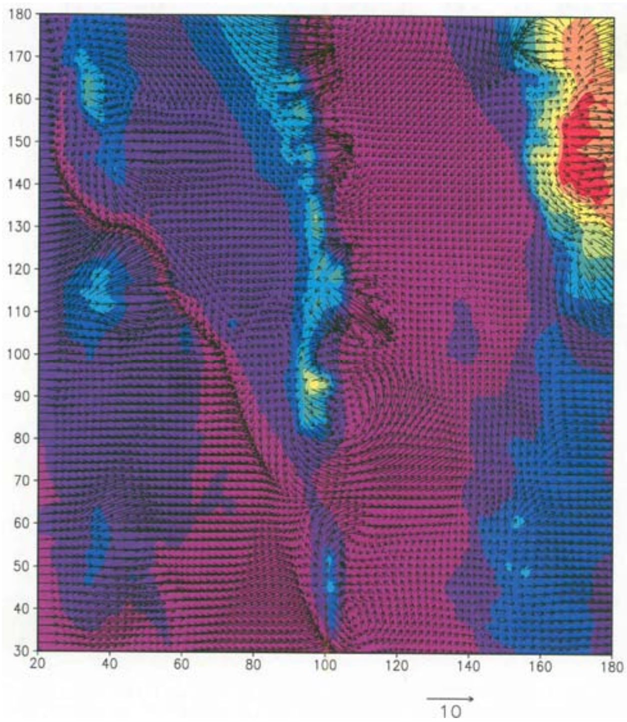

(a) surface wind field

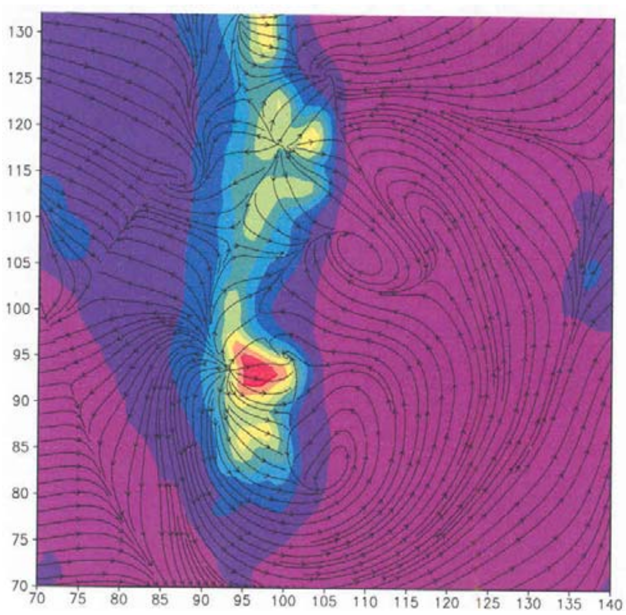

(b) streamlines

Fig. 9: NTU/P model predictions of (a) surface wind field and (b) streamlines for the case of an initial 5 m/s westerly prevailing wind at WSMR (after 2.5 hours of model integration); terrain levels (m) are indicated by color contour regions.

near the Organ Mountains is limited, and additional measurements would be required to fully reveal the actual flow. The kinds of blocking predicted by the NTU/P model has also been seen in the observational results for westerly and southwesterly flow cases in which the Froude Number was less than 0.5. During the January to March 2004 observations, fully and partially blocked flow, as well as lee waves and hydraulic jumps in the lee of mountains, were recorded.

5. SCALABILITY RESULTS

As indicated in Section 2, the NTU/P model software package has been fully parallelized using Message Passing Interface (MPI) library routines. To evaluate the scalability characteristics of this advanced forecasting model, we ran the case described in Subsection 4.1 (down-slope wind storm case at WSMR on January 25, 2004) on the unclassified 1024-node Linux Networx Evolocity II cluster at the ARL MSRC. Maintaining a fixed problem size of four million grid points (200x200x100), we varied the number of processors from 4 to 128 and ran the test case for three hours of simulation time. Table 1 shows the total wall clock times, speed-up factors (relative to the 4-processor case), and percentages of optimum speed-up achieved for the various numbers of processors. As the table indicates, the NTU/P model scales very well on the ARL MSRC's Linux cluster.

Table 1. Scalability Results for NTU/P Model

Number of Processors	Wall Clock Time (s)	Actual Speed-up Factor	Optimum Speed-up Factor	% of Optimum Speed-up
4	78523	reference	--	--
8	40287	1.95	2	97.5
16	20925	3.75	4	93.8
32	11114	7.07	8	88.3
64	5998	13.09	16	81.8
128	3658	21.47	32	67.1

CONCLUSIONS

The NTU/P model was applied to several well-observed real terrain cases for the Organ and San Andres Mountains in southern New Mexico. On January 25, 2004, a down-slope wind storm in the lee of these mountains was accompanied by a hydraulic jump and lee waves, all of which were well-observed. The NTU/P model was initialized with the 12Z El Paso sounding for January 25 and run for several hours. As shown, the model successfully predicted much of the atmospheric phenomena observed on that day. The model was also applied to partially and fully blocked flow conditions on the WSMR terrain. With a Froude Number of less than 0.5, the model shows that the terrain causes pronounced blocking, along with the formation of a lee vortex. The model-predicted surface wind fields are consistent with the local WSMR surface flows observed for these kinds

of conditions. On January 19, 2004, the WSMR surface observations showed super- and sub-critical flows. The NTU/P model was initialized with the 12Z El Paso sounding for January 19 and run for several hours. The model's predicted wind flow agrees fairly well with the intricacies of the complex flow that were actually observed.

Knowing the surface and boundary layer wind fields benefits the Army in several important ways. The characterization of dispersion and diffusion of various biological/chemical agents in the battlefield requires detailed information including wind speed, wind direction, and the variability of both, all of which can be reliably provided by high resolution numerical modeling. Also, some munitions are significantly affected by the low-level wind field as they maneuver in acquiring and engaging their target; obtaining a reliable forecast of the target area wind field will allow them to be more optimally aimed. In addition, the low-level wind and turbulence fields are linked; hence, knowing where to avoid severe turbulence and adverse winds will greatly benefit Army aviation missions, especially those involving helicopters, unmanned aerial vehicles, and para-drop operations. Finally, the wind environment and embedded turbulence significantly affect acoustic propagation, so accurate numerical forecasts of wind and turbulence fields will help acoustic detection and avoidance programs.

While the results presented in this paper demonstrate the feasibility of producing high resolution forecasts of complex wind flow caused by and occurring in proximity to mountainous terrain, much additional work remains to be done. The NTU/P model used here was found to have high scalability characteristics, so that with the model domain used in this paper, it is possible to obtain the forecast results over 21 times faster using 128 processors versus use of only 4. This means that a three hour forecast can be completed in about an hour. If a semi-implicit approach is implemented to solve the vertical momentum equation, and higher computational efficiency is attained, it should be possible to more than halve the NTU/P model's run time. The ARL MSRC will soon be installing a new Linux Networx Advanced Technology Cluster with 1122 dual-core compute nodes. This significant increase in computing power will enable us to generate more detailed weather forecasts using even higher resolution grids (e.g., 100-m grid point spacing, with billions of grid points) for regions with complex terrain. This will help us determine the levels of detail and accuracy that can be achieved using the currently available (state-of-the-art) numerical weather forecasting models. While increased grid resolution (i.e., smaller grid spacing) may lead to more accurate forecasts, it may also reveal model deficiencies that can be corrected, or at least improved. As computing power continues to increase, we anticipate that a practical numerical weather forecasting tool will eventually be developed for use in the field. The ultimate goal of this work is to provide Army commanders with accurate assessments of meteorological conditions in the battlefield (in near real-time) to assist in their strategic planning and decisions.

ACKNOWLEDGEMENTS

This work was supported in part by a grant of computer time from the DoD High Performance Computing Modernization Program (HPCMP) at the ARL MSRC, Aberdeen Proving Ground, MD.

REFERENCES

Chern, J. D., 1994: Numerical simulations of cyclogenesis over the western United States, Ph. D. Thesis, Department of Earth and Atmospheric Sciences, Purdue University, 178 pp.

Gadd, A. J., 1978: A split explicit integration scheme for numerical weather prediction. Quart. J. Roy. Met. Soc., 104, 569-582.

Grove, D. J., and P. A. Haines, 2002: Fine scale numerical prediction of atmospheric flow in complex terrain. 2002 DRI Report, US Army Research Laboratory, Adelphi, MD.

Haines, P. A., J. D. Chern. and W. Y. Sun, 1997: Numerical simulation of the Valentine's Day storm during WISP 1990. Tellus, 49A. 595-612̃.

Hsu, W. R., and W. Y. Sun, 2001: A time-split, forward-backward numerical model for solving a nonhydrostatic and compressible system of equations. Tellus, 53A, 279-299.

Scorer, R. S., 1949: Theory of waves in the lee of mountains. Quart. J. Roy. Meteor. Soc., 75, 41-56.

Sun, W. Y., 1993: Numerical experiments for advection equation. J. of Comput. Phys., 108, 264-271.

Sun, W. Y., and J. D. Chern, 1993: Diurnal variation of lee-vortexes in Taiwan and surrounding area. J. Atmos. Sci. 50, 3404-3430.

USE OF HIGH PERFORMANCE COMPUTING TO CONDUCT FINE SCALE NUMERICAL SIMULATIONS OF ATMOSPHERIC FLOW IN COMPLEX TERRAIN

D. J. Grove
U. S. Army Research Laboratory
Aberdeen Proving Ground, MD 21005-5067

P. A. Haines
U. S. Army Research Laboratory
White Sands Missile Range, NM 88002

W. Sun
Purdue University
West Lafayette, IN 47907-2051

W. Hsu
National Taiwan University
Taipei, Taiwan

25th Army Science Conference
Orlando, FL
November 27 – 30, 2006

OBJECTIVE

Evaluate the capabilities of a nonhydrostatic model to predict weather conditions in complex terrain for the U. S. Army

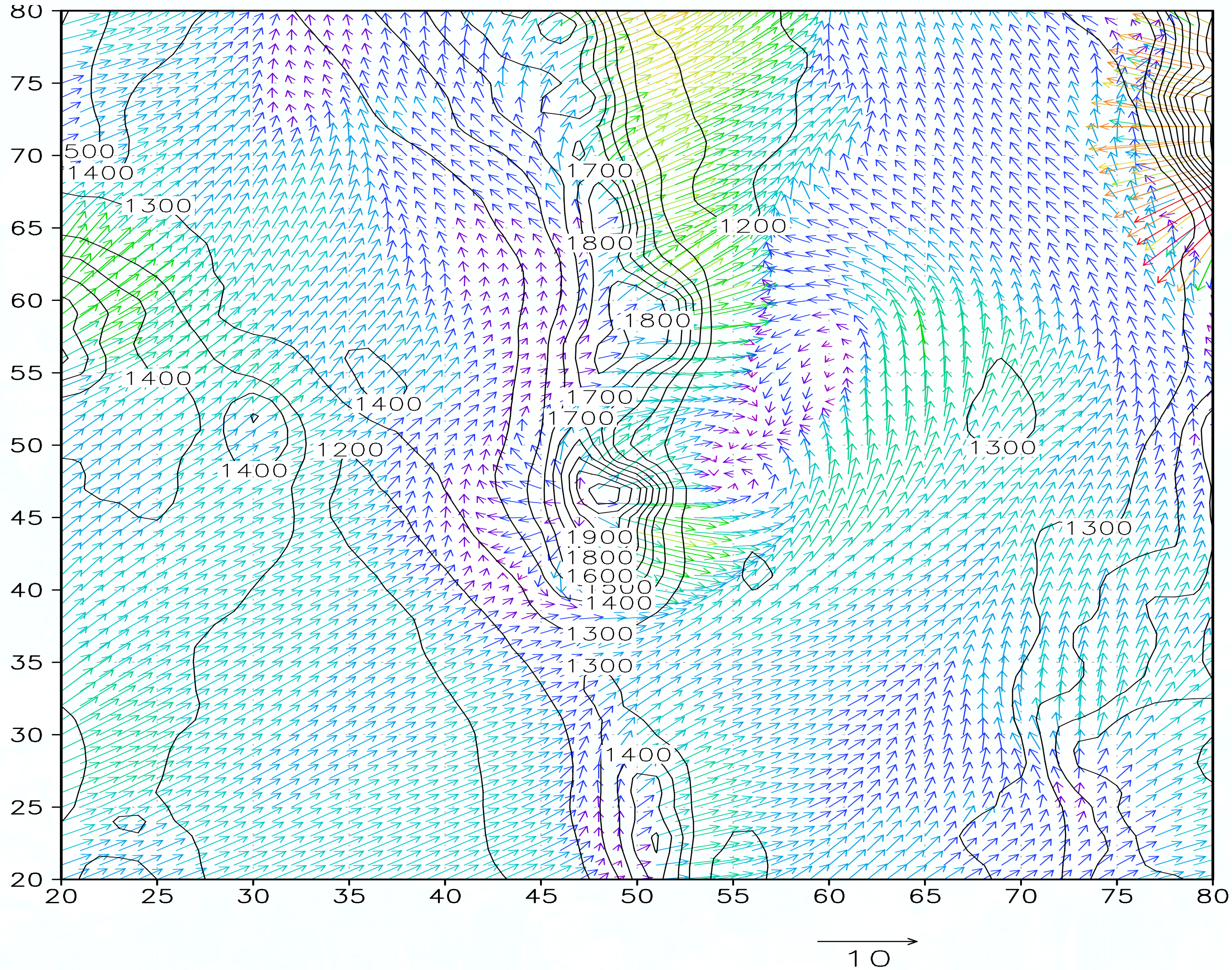

Organ Mountains, NM

NTU/Purdue Nonhydrostatic Model

- 3-D Fully Explicit, Non-Hydrostatic, Compressible Equations (Hsu and Sun, *Tellus A* 53 (3), 2001). θ_e, ρ, q_w, u, v, w.

- Double Forward-Backward Time Integration procedure for treating both sound waves and internal gravity waves . Uses the time-splitting approach for the gravity wave and advective steps.

- Uses a terrain following vertical grid that is consistent with the Purdue Regional Model, so it can use already developed physical parameterizations for the ground surface, microphysics, and radiative transfer.

- Solves the density tendency equation instead of the pressure tendency equation; no diabatic term.

NTU/Purdue Model Domain (WSMR)

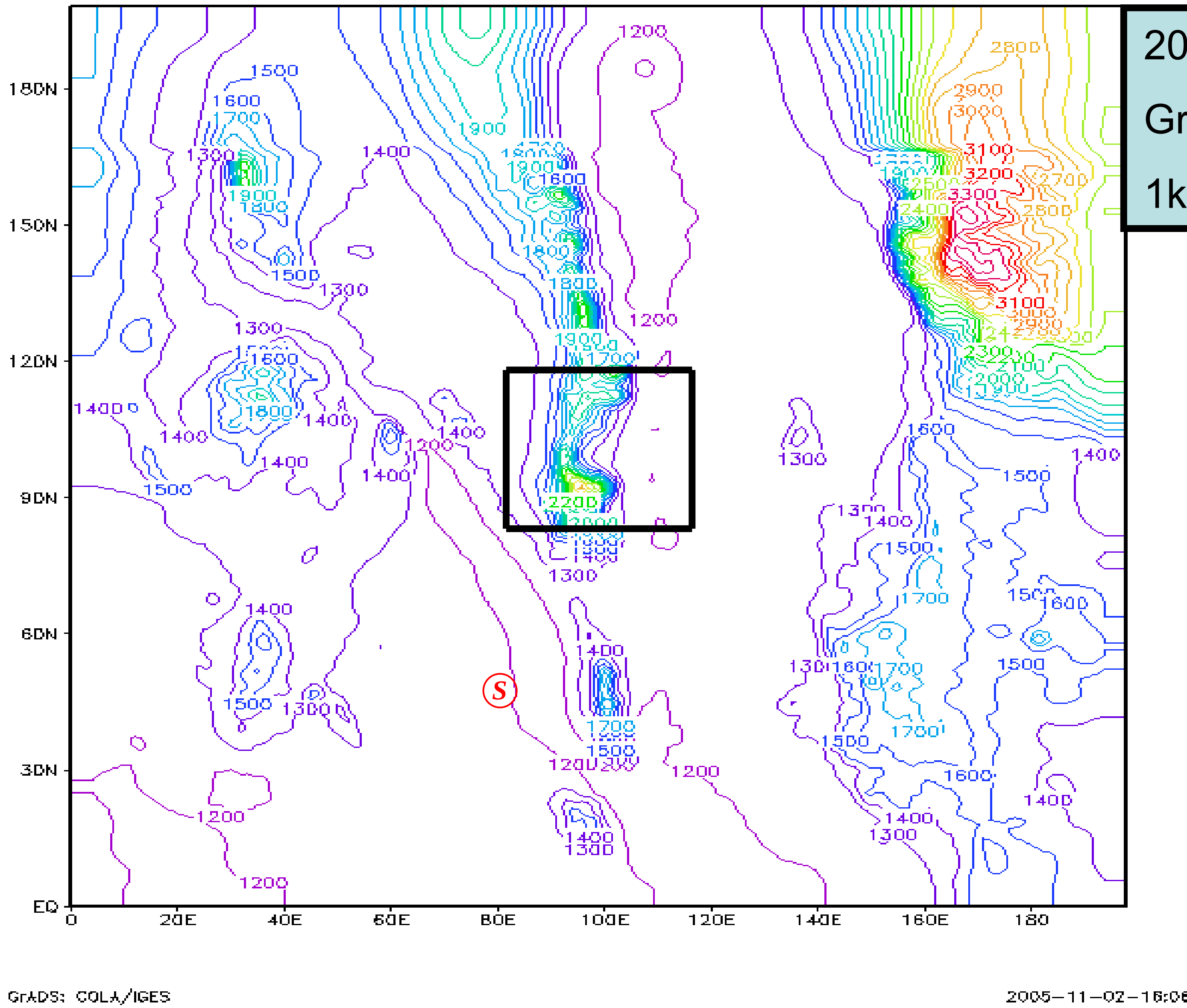

201 x 201

Grid @

1km Δ**x**, Δ**y**

Local Terrain Details

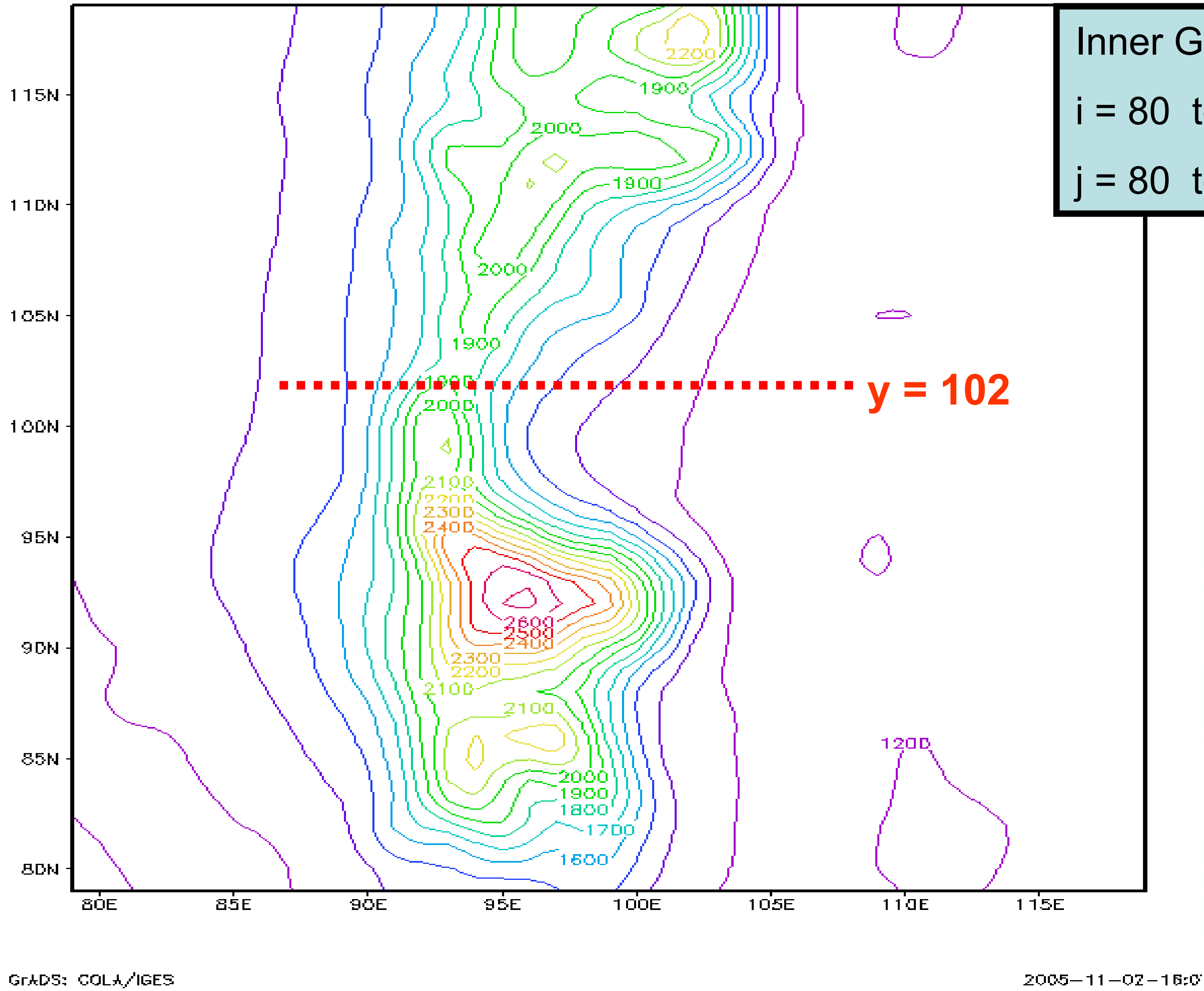

Inner Grid area

i = 80 to 120

j = 80 to 120

Summary of NTU/Purdue Model Results

- Numerical forecasts of wind flow were generated for two different dates: 01-25-2004 and 01-19-2004.
- NTU/Purdue model was initialized with the El Paso 12Z soundings from those dates, and then integrated for 3 - 4 hours to obtain numerical forecasts of the wind flow.
- Model results were compared to Meso-γ and WSMR Surface Atmosphere Measuring System (SAMS) wind and pressure observations, the White Sands Profiler, and other data.
- For the 01-25-2004 case, both the model and observations indicate strong downslope winds, a stationary wave train extending downwind from the mountains, and (apparently) a hydraulic jump.
- For the 01-19-2004 case, both the model and observations show blocked flow in the lee of the Organ mountains and downslope flow to the north of the WSMR post area.

El Paso Sounding for 12 Z on January 25, 2004

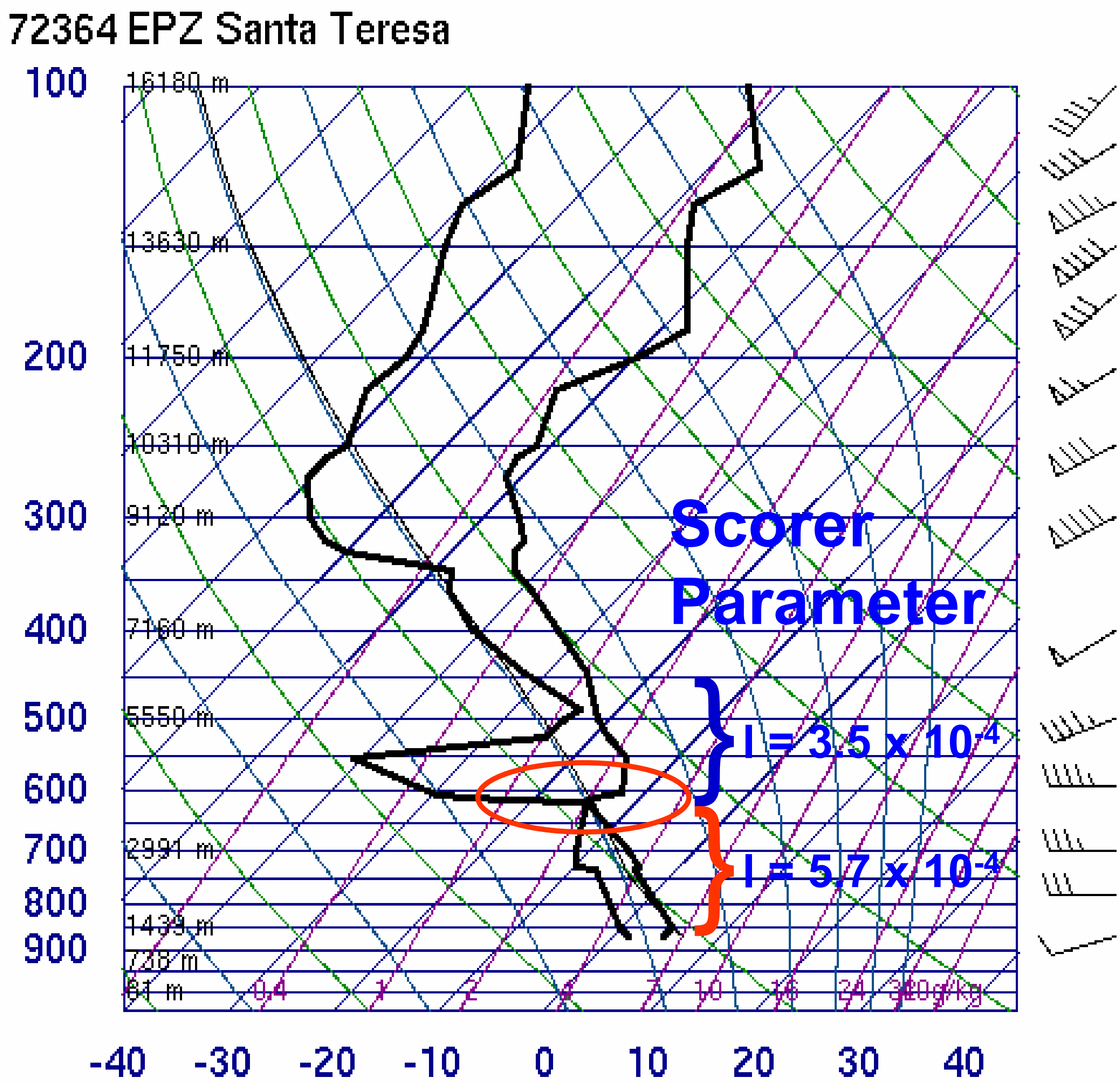

Comparison of Model Predictions with Observed WSMR Pressure Perturbations at 0800 on January 25, 2004

Color Lines:
Purdue/NTU NH Model Pressure Perturbations (Pascals) 0 to -200

Dark Bold Numbers:
Observed Pressure Perturbations

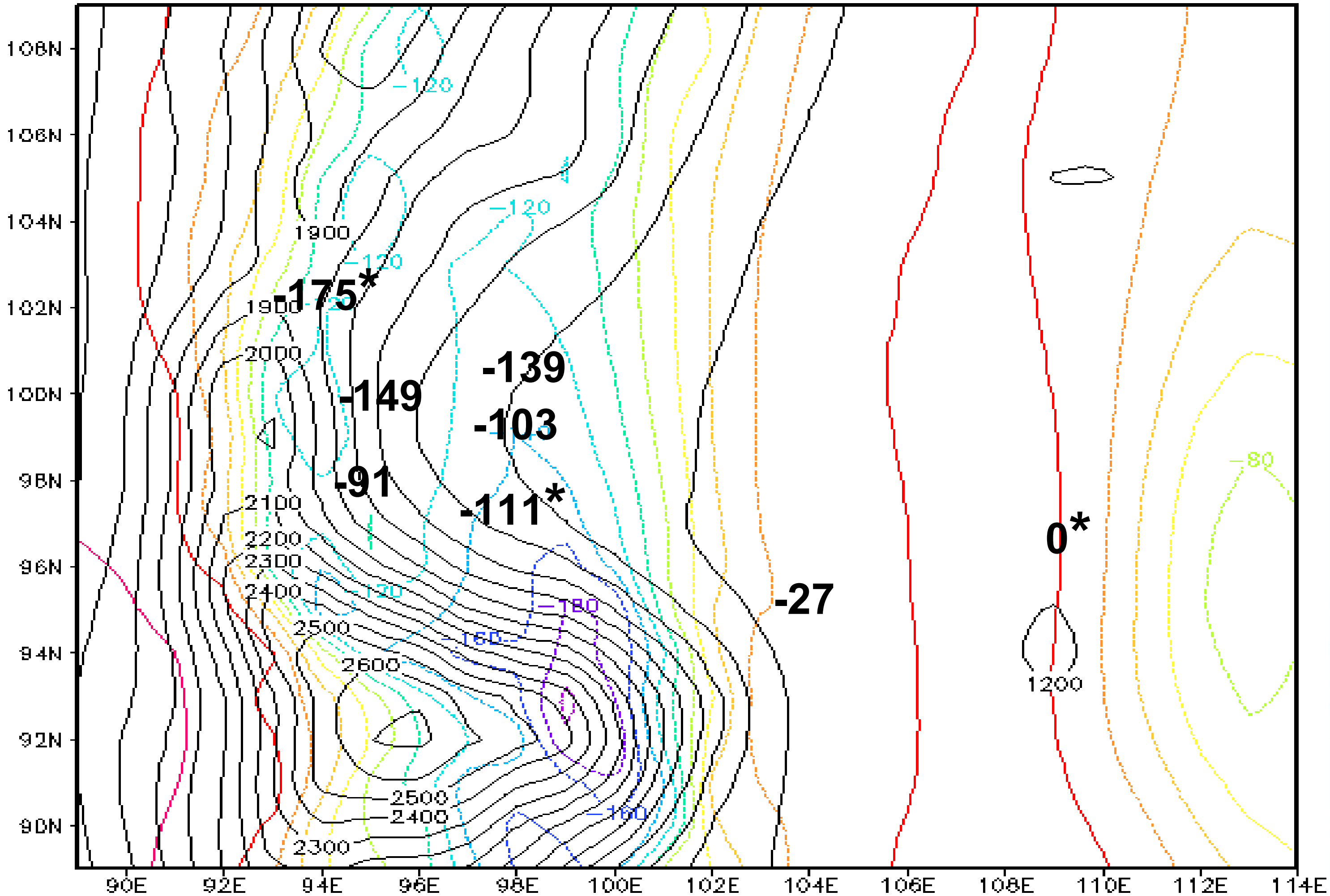

Grid number west to east direction → E

GrADS: COLA/IGES 2005-11-02-1

Comparison of Model Predictions with Observed WSMR 10 m Wind Field at 0800 on January 25, 2004

Wind Barbs:
Purdue/NTU NH Model

Dark Arrows:
Observed Winds

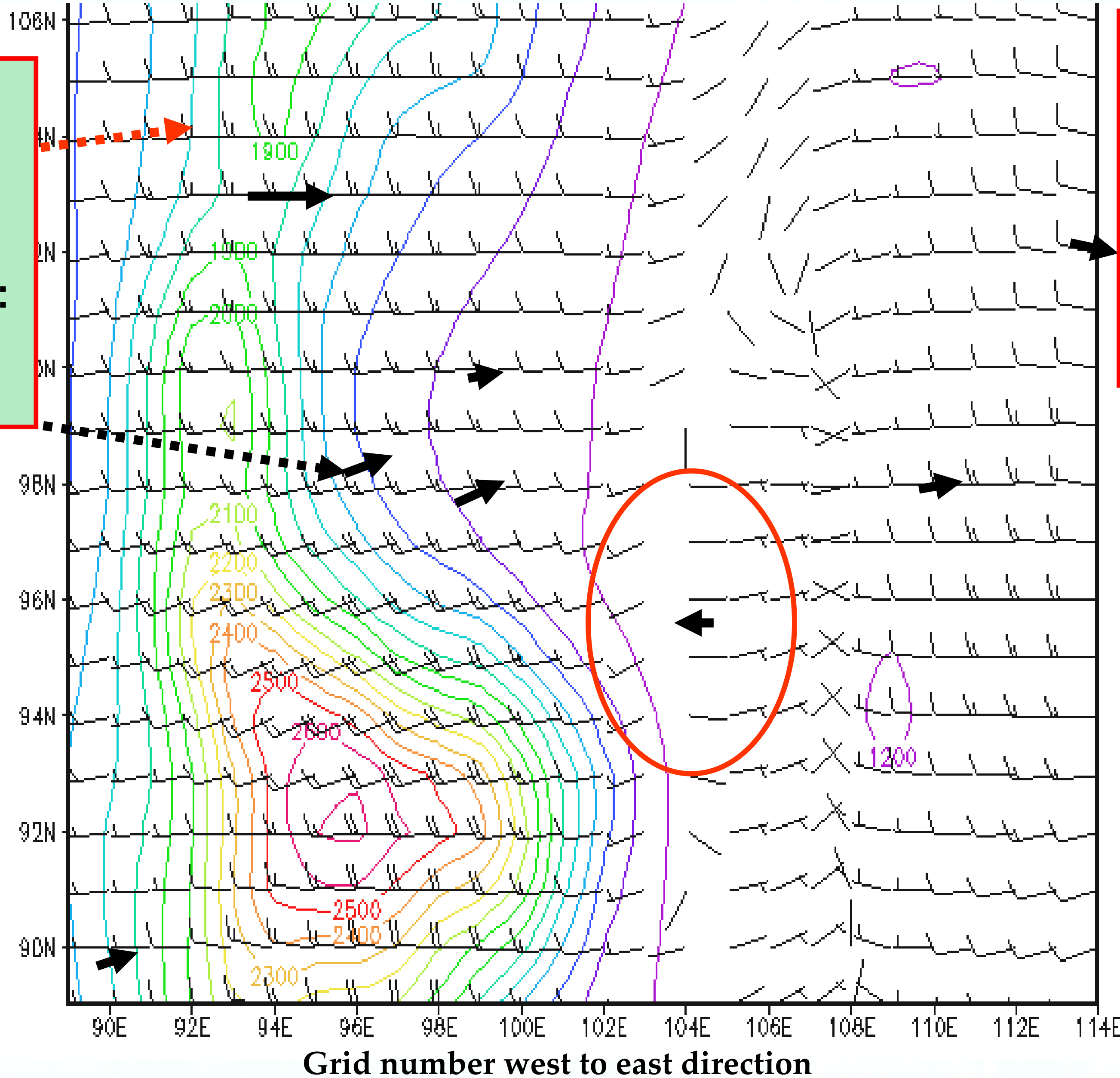

201x201 grid 1km Grid spacing. This plot shows the central part of the model domain

Color contours show the model terrain in m asl.

Comparison of Model Predictions with Observed WSMR 10 m Wind Field at 0800 on January 25, 2004

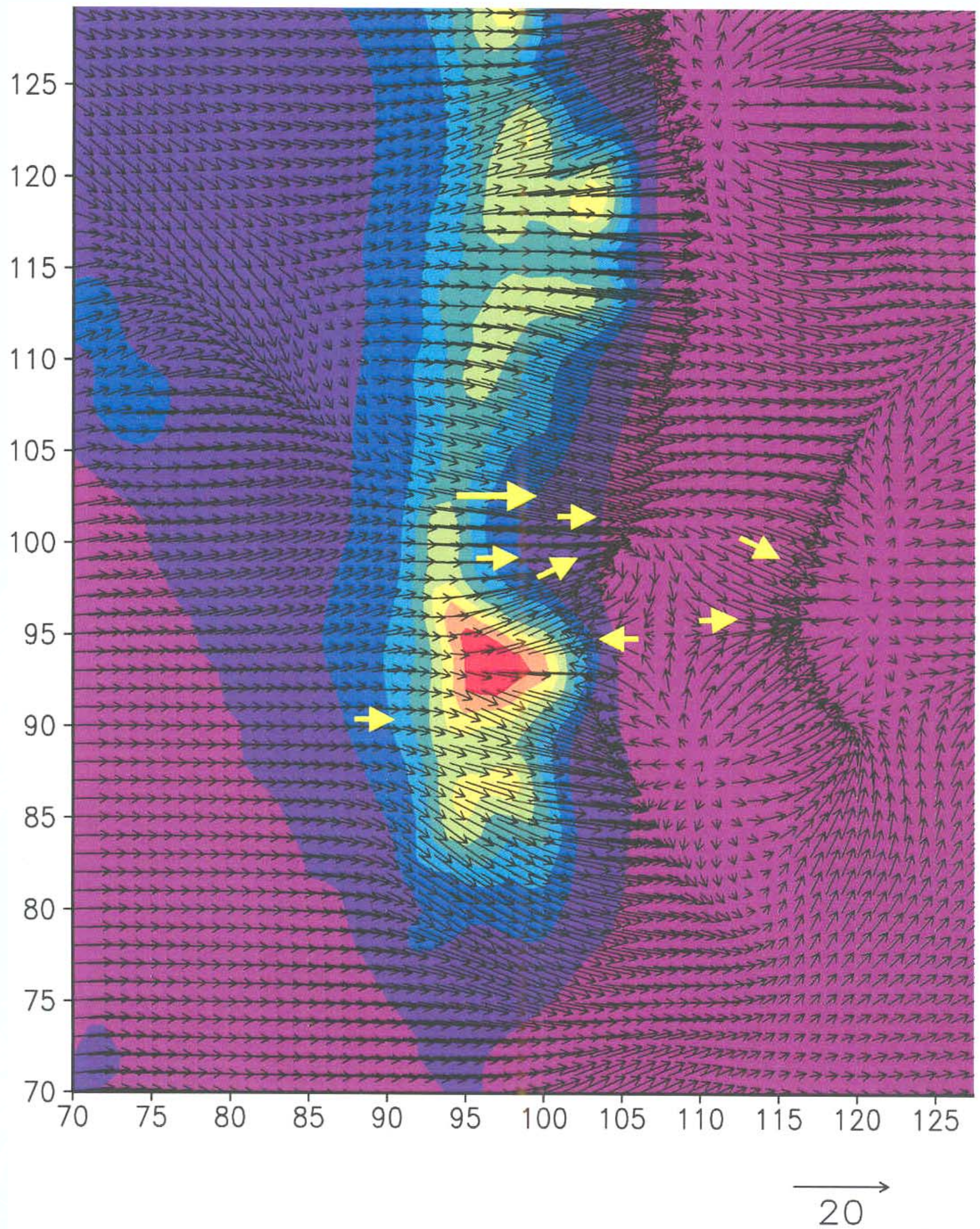

Model-Predicted Vertical Velocity Field at y=102

This cross-section includes the WSMR Wind Profiler (dark line). The vertical velocities (m/sec) show the trapped lee waves extending eastward away from the mountains. The altitude (m) is shown on the left edge of this figure

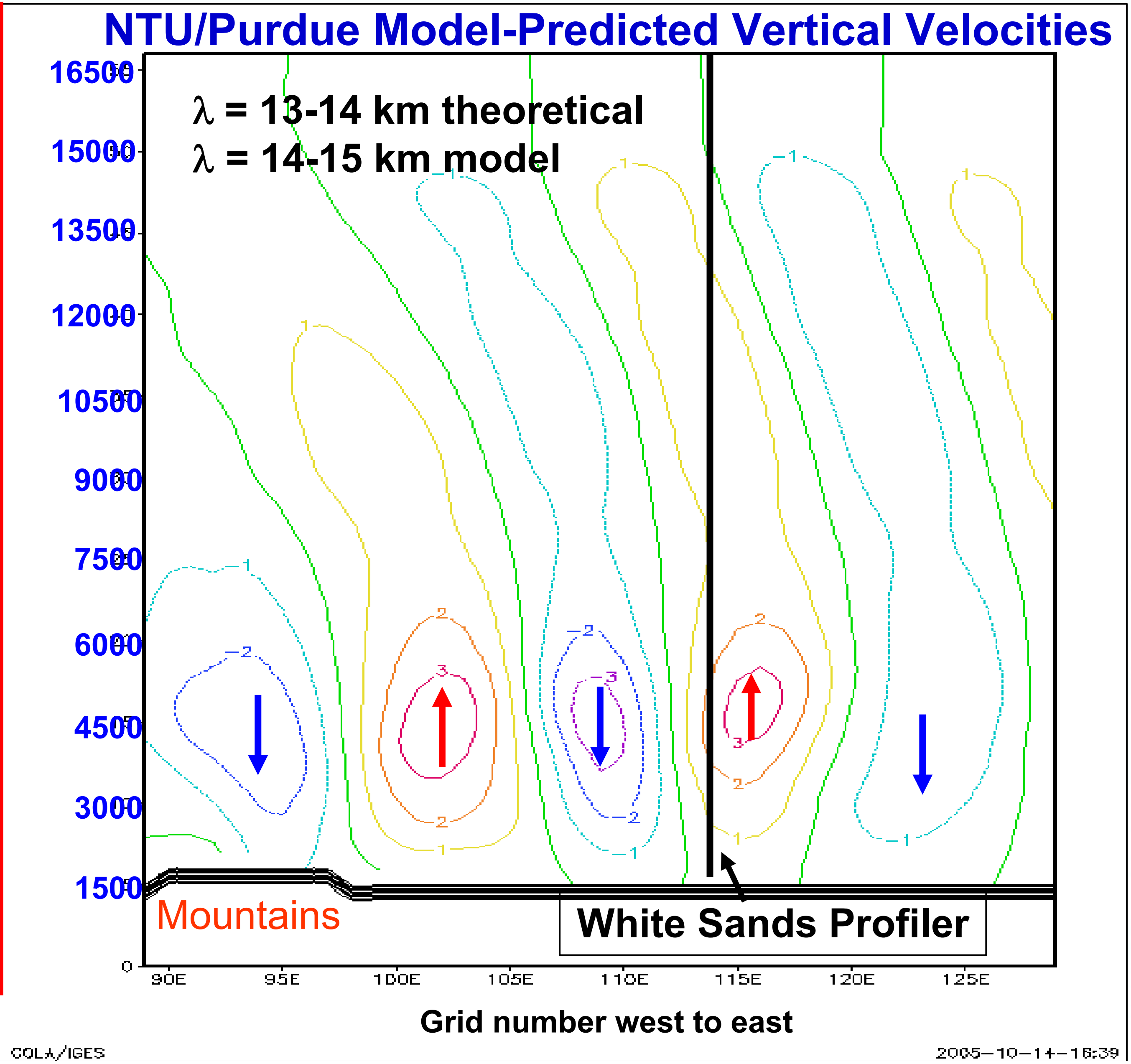

Comparison of Model-Predicted Vertical Velocity Profiles with Observations from WSMR Wind Profiler on 01-25-2004

NTU/Purdue model vertical velocities (connected lines)

Wind Profiling Radar observed vertical velocities (+ and #) with 0.5 m/s error bars.

The vertical scale is altitude in meters asl

Average terrain height upwind

Elevation of Basin Floor

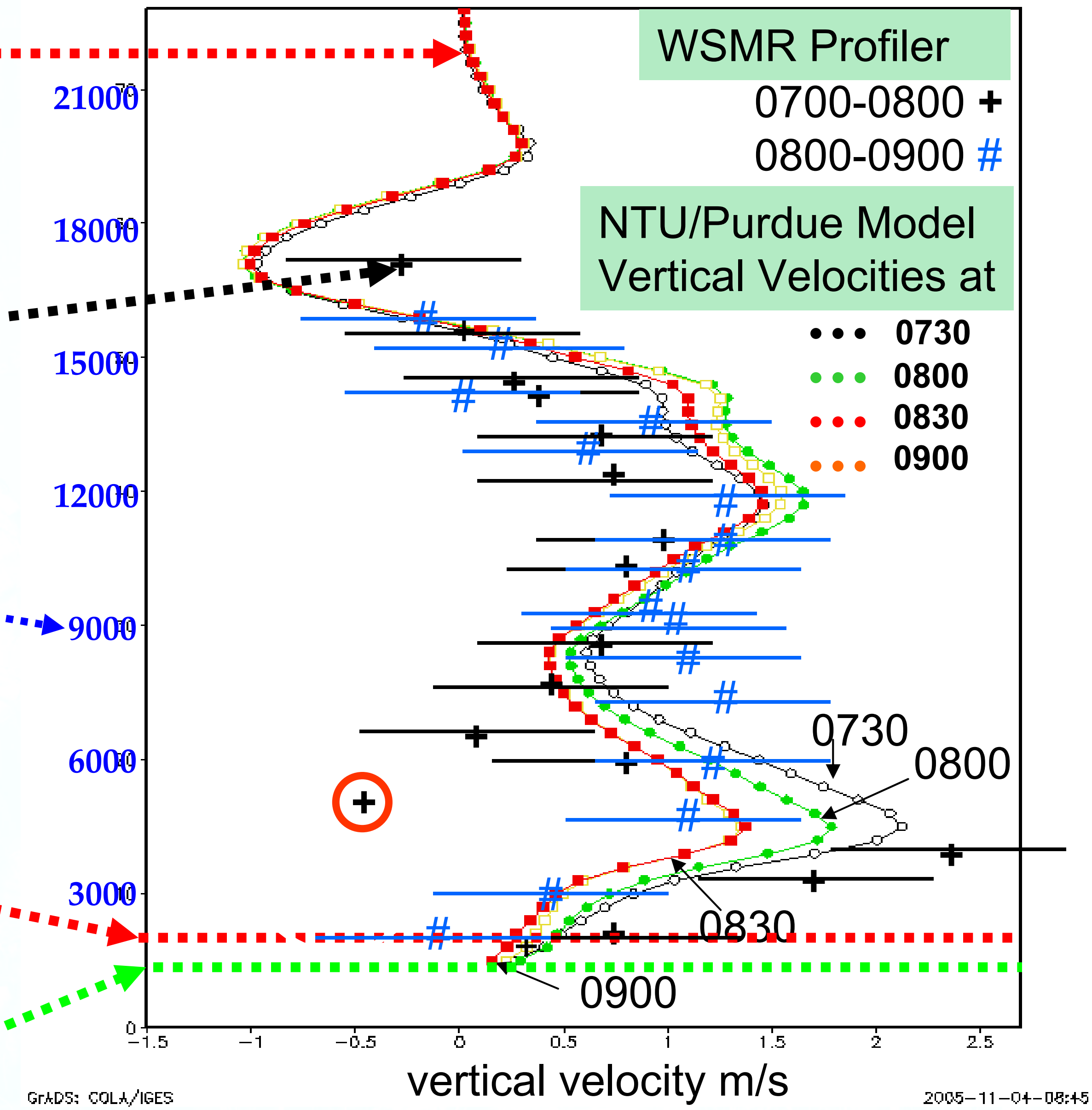

El Paso Sounding for 12 Z on January 19, 2004

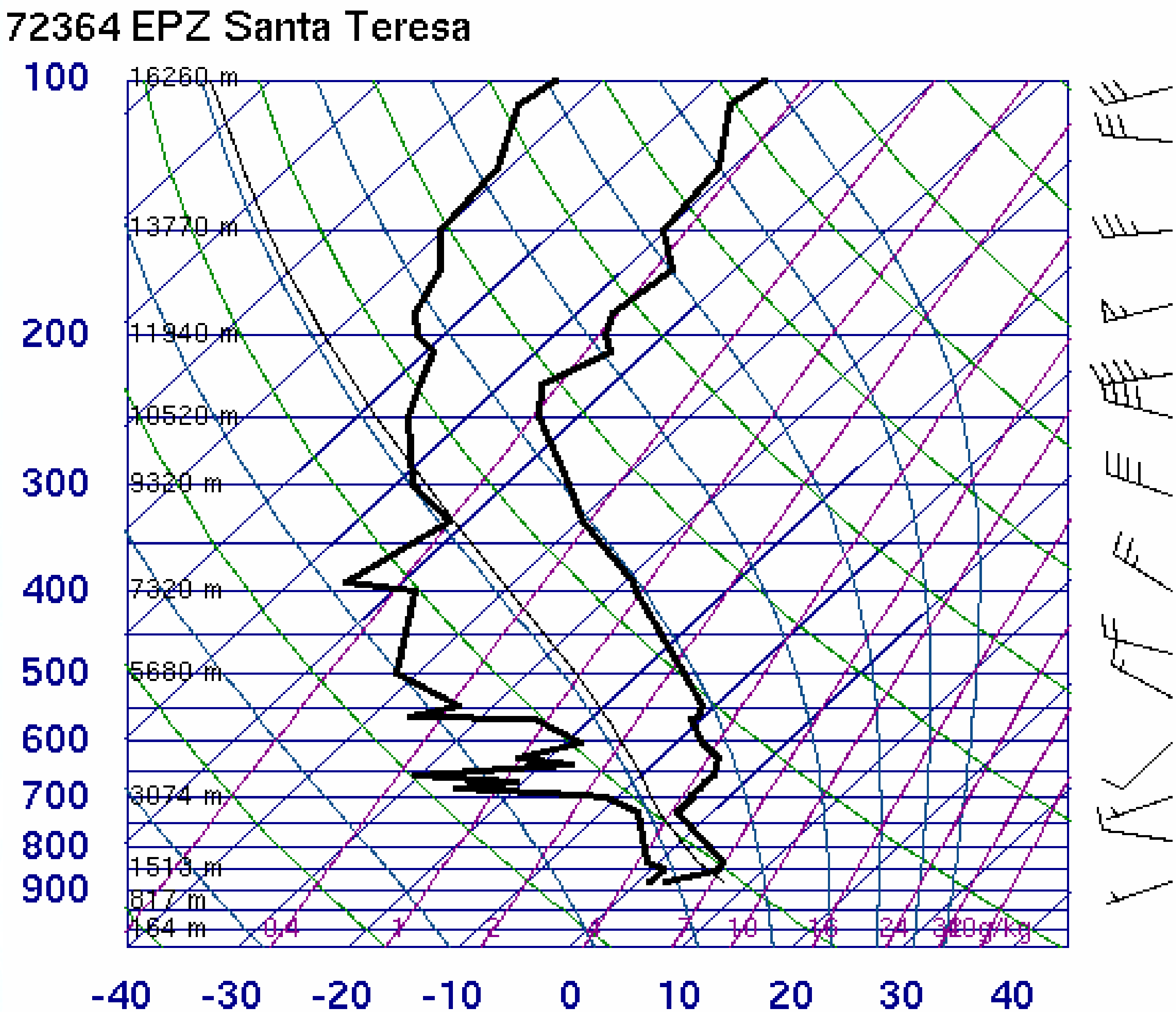

Comparison of Model Predictions with Observed WSMR 10 m Wind Field at 0800 on January 19, 2004

Wind Vectors:
NTU/ Purdue NH Model

Dark Arrows:
Observed Winds

Froude Number, FN
FN = U/Nh where
U = wind speed
N = Brunt-Vaisala Frequency
h = terrain height

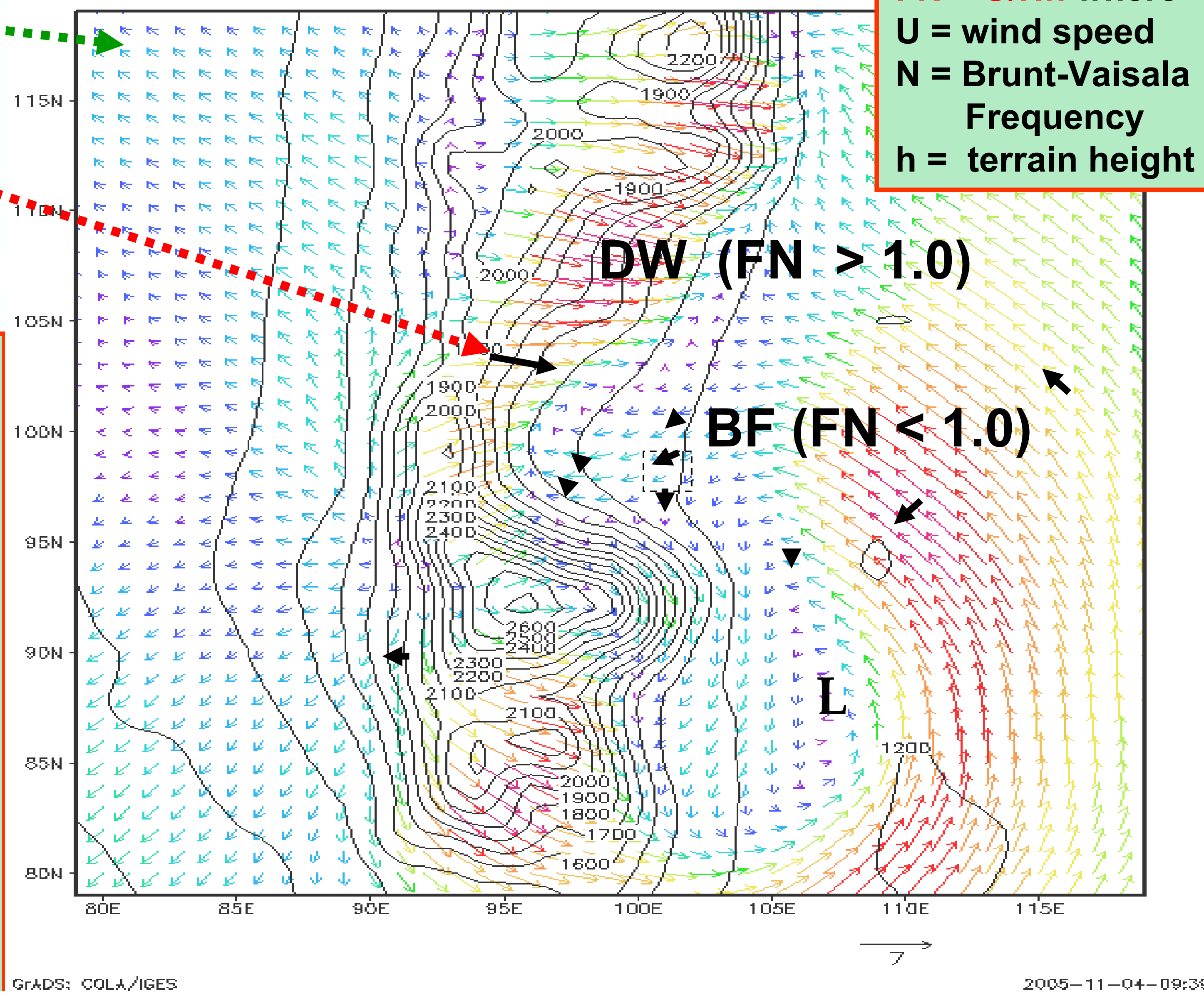

The low-level flow shows a lee vortex (L) east of the Mountains, blocked flow (BF) to its north, and downslope wind (DW) on the lee north of WSMR post. All are consistent with the local flow's Froude number.

Scalability Results

Number of Processors	Wall Clock Time (s)	Actual Speed-up Factor	Optimum Speed-up Factor	% of Optimum Speed-up
4	78523	reference	--	--
8	40287	1.95	2	97.5
16	20925	3.75	4	93.8
32	11114	7.07	8	88.3
64	5998	13.09	16	81.8
128	3658	21.47	32	67.1

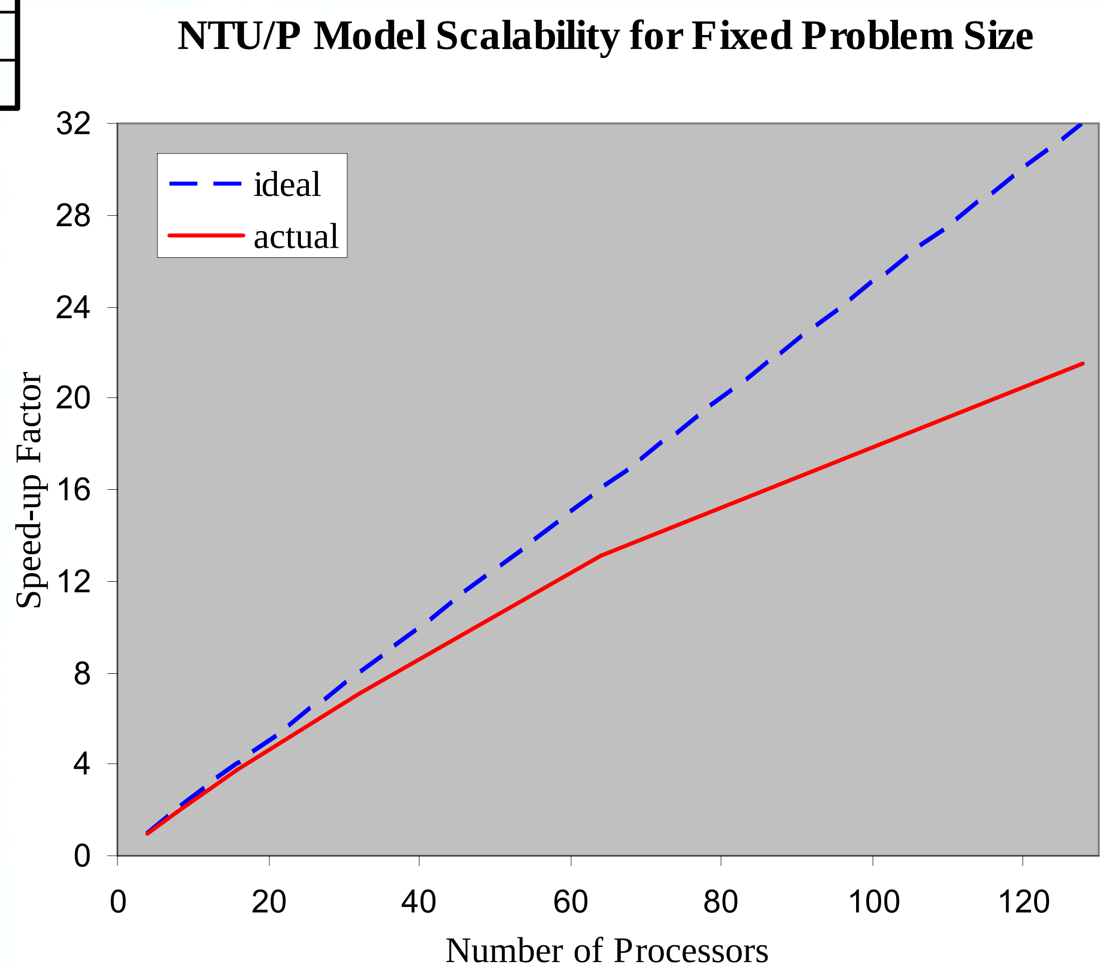

CONCLUSIONS

- **The NTU/Purdue model was run for two well-observed WSMR cases.**
  - The model successfully generated a hydraulic jump signature for the lee wave case.
  - For the case with juxtaposition of super- and sub-critical flow, the model's wind flow agreed fairly well with the observations.

- **The model results demonstrate that it is possible to forecast the details of flow in complex terrain.**

- **The numerical implementation of the model scales fairly well (up to 128 processors) for the cases presented.**

Potential Benefits/Applications

- Improved forecasts of dispersion and diffusion characteristics of various biological/chemical agents in the battlefield

- Improved success rate for Army aviation missions, especially those involving helicopters, unmanned aerial vehicles, and para-drop operations

- Improved aiming of munitions that are significantly affected by the low-level wind field

- Improved characterization of acoustic propagation in the battlefield

- **Ultimate Goal:** to provide Army commanders with more accurate assessments of meteorological conditions in the battlefield (in near real-time) to assist in their strategic planning and decisions